JPET Fast Forward. Published on June 7, 2011 as DOI: 10.1124/jpet.111.183210

JPET#183210

Resveratrol ameliorates muscular pathology in the dystrophic mdx mouse, a model for Duchenne muscular dystrophy

Yusuke S. Hori, Atsushi Kuno, Ryusuke Hosoda, Masaya Tanno, Tetsuji Miura, Kazuaki Shimamoto and Yoshiyuki Horio

Department of Pharmacology (Y. S. H., A. K., R. H., Y. H.) and Second Department of Internal Medicine (A. K., M. T., T. M., K. S.) School of Medicine, Sapporo Medical University, Sapporo 060-8556, Japan

Running Title Page

Treatment of muscular dystrophy by resveratrol

Yoshiyuki Horio, M.D., Ph.D.
Department of Pharmacology,
Sapporo Medical University,
S1 W17, Chuo-ku, Sapporo 060-8556, Japan.
Tel.: + 81 11 611 2111;
Fax: + 81 11 612 5861;
E-mail: horio@sapmed.ac.jp

Number of text pages: 39
Number of tables: 0
Number of Figs: 8
Number of references: 34
Number of words in the abstract: 244
Number of words in the Introduction: 647
Number of words in the Discussion: 1493

ABBREVIATIONS: α-SMA, α-smooth muscle actin; CK, creatine kinase; CM-H_2DCFDA, 5-(and-6)-chloromethyl-2',7'-dichlorodihydrofluorescein diacetate acetyl ester; DMD, Duchenne muscular dystrophy; GAPDH, glyceraldehydes 3-phosphate dehydrogenase; IL-1β, interleukin-1β; LDH, lactate dehydrogenase; Nox, NADPH oxidase; 8-OHdG, 8-hydroxy-2'-deoxyguanosine; PBS, phosphate-buffered saline; qRT-PCR, quantitative reverse transcription polymerase chain reaction; PGC-1α, peroxisome proliferators-activated receptor-gamma coactivator 1α; ROS, reactive oxygen species; Sir2, silent mating type information regulation 2; siRNA, small interfering RNA; Sod, superoxide dismutase; TGF-β, transforming growth factor-beta; TNF-α, tissue necrosis factor-α.

Section: Drug Discovery and Translational Medicine

JPET Fast Forward. Published on June 7, 2011 as DOI: 10.1124/jpet.111.183210
This article has not been copyedited and formatted. The final version may differ from this version.

ABSTRACT

Muscular dystrophies are inherited myogenic disorders accompanied by progressive skeletal muscle weakness and degeneration. We previously showed that resveratrol (3,5,4'-trihydroxy-trans-stilbene), an anti-oxidant and activator of the NAD^+-dependent protein deacetylase SIRT1, delays the progression of heart failure and prolongs the lifespan of δ-sarcoglycan-deficient hamsters. Because a defect of dystroglycan complex causes muscular dystrophies, and δ-sarcoglycan is a component of this complex, we hypothesized that resveratrol might be a new therapeutic tool for muscular dystrophies. Here we examined resveratrol's effect in mdx mice, an animal model of Duchenne muscular dystrophy. Mdx mice that received resveratrol in the diet for 32 weeks (4 g/kg diet) showed significantly less muscle-mass loss and non-muscle interstitial tissue in the biceps femoris compared with mdx mice fed a control diet. In the muscles of these mice, resveratrol significantly decreased oxidative damage shown by the immunostaining of nitrotyrosine and 8-hydroxy-2'-deoxyguanosine and suppressed the up-regulation of NADPH oxidase subunits Nox4, Duox1, and $p47^{phox}$. Resveratrol also reduced the number of α-smooth muscle actin $(\alpha\text{-SMA})^+$ myofibroblast cells and endomysial fibrosis in the biceps femoris, although the infiltration of $CD45^+$ inflammatory cells and increase in TGF-β1 were still observed. In C2C12 myoblast cells, resveratrol pretreatment suppressed the TGF-β1-induced increase in

JPET Fast Forward. Published on June 7, 2011 as DOI: 10.1124/jpet.111.183210
This article has not been copyedited and formatted. The final version may differ from this version.

reactive oxygen species, fibronectin production, and expression of α-SMA, and SIRT1 knockdown blocked these inhibitory effects. SIRT1 siRNA also increased the expression of Nox4, $p47^{phox}$, and α-SMA in C2C12 cells. Taken together, these findings indicate that SIRT1 activation may be a useful strategy for treating muscular dystrophies.

JPET Fast Forward. Published on June 7, 2011 as DOI: 10.1124/jpet.111.183210
This article has not been copyedited and formatted. The final version may differ from this version.

Introduction

Muscular dystrophies are hereditary diseases involving progressive muscular weakness and the degeneration of muscle cells (Emery, 2002). Loss-of-function mutations in genes encoding components of the dystroglycan complex, such as dystrophin and sarcoglycans, result in increased fragility of the sarcolemma. The mechanism leading to muscular injury remains unknown. Duchenne muscular dystrophy (DMD), caused by dystrophin deficiency, is the most prevalent lethal X-linked myopathy, and it is severe. The dystrophin-deficient mdx mouse is used as a DMD model, although it retains a normal lifespan and the resultant myopathology is much less severe compared to the human disease course. Several pharmacological treatments for DMD have been studied, including exon skipping (Alter et al., 2006) and activation of the nitric oxide-cGMP signaling pathway by a phosphodiesterase 5 inhibitor (Asai et al., 2007). However, only corticosteroids are currently used as an established therapy.

Since oxidative damage is found in the muscle even before the onset of muscle necrosis (Disatnik et al., 1998), reactive oxygen species (ROS) have been implicated in the pathogenesis of DMD (Rodriguez and Tarnopolsky, 2003). Administration of the antioxidant N-acetylcysteine to mdx mice decreases the ROS levels, significantly ameliorates stretch-induced muscle damage, and reduces the number of centrally nucleated premature

muscle fibers (Whitehead et al., 2008). Inflammatory cells, such as neutrophils and macrophages, may be one of the sources of excessive ROS in the dystrophic muscle. Myofiber necrosis promotes the invasion of inflammatory cells, releases cytokines such as transforming growth factor β (TGF-β), and enhances myofiber degeneration. TGF-β induces the transformation of fibroblasts into myofibroblasts, which extensively promote fibrosis by secreting collagens and fibronectin (Barnes and Gorin, 2011). Inhibition of the TGF-β signal and inflammatory response is a therapeutic strategy for DMD (Huang et al., 2009; Taniguti et al., 2010).

Sirtuins are mammalian homologues of Sir2 (silent mating type information regulation 2), which is implicated in the longevity of yeast, warms, and flies (Horio et al., 2011). Of the seven mammalian sirtuins, SIRT1 is an NAD^+-dependent histone/protein deacetylase that plays crucial roles in cell survival, oxidative stress reduction, inflammation inhibition, metabolism, differentiation, and DNA repair (Horio et al., 2011). Resveratrol (3,5,4'-trihydroxy-trans-stilbene), a naturally occurring polyphenol found in grapes and red wine, has been found to activate SIRT1 (Howitz et al., 2003). We found that SIRT1 is a nucleocytoplasmic shuttling protein (Tanno et al., 2007). Its translocation into the nucleus induces superoxide dismutase 2 (Sod2/Mn-Sod), decreases ROS levels, and inhibits oxidative stress-induced cell death in C2C12 myoblast cells (Tanno et al., 2010). The administration of

JPET Fast Forward. Published on June 7, 2011 as DOI: 10.1124/jpet.111.183210
This article has not been copyedited and formatted. The final version may differ from this version.

resveratrol to TO-2 hamsters, an animal model of congenital heart failure, increases the expression level of cardiac Sod2, decreases fibrosis, ameliorates cardiac dysfunction, and extends the lifespan (Tanno et al., 2010). Dilated cardiomyopathy develops in TO-2 hamsters because of a mutation in δ-sarcoglycan, a component of the dystroglycan complex.

Collectively, these findings raised the possibility that the activation of SIRT1 might also be effective in treating muscular dystrophies. In addition, SIRT1 deacetylates and activates a peroxisome proliferator-activated receptor-gamma coactivator-1α (PGC-1α) (Rodgers et al., 2005), which inhibits muscular atrophy induced by denervation and is involved in muscle fiber-type switching from glycolytic fast fibers to oxidative slow fibers (Sandri et al., 2006; Schuler et al., 2006). In addition, PGC-1α induces Sod2 and reduces ROS levels (St-Pierre et al., 2006). The overexpression of PGC-1α in the muscle cells of mdx mice reduces muscle fiber damage, increases the running performance, and decreases the serum creatine kinase (CK) level (Handschin et al., 2007), indicating that SIRT1's activation by resveratrol might also provide an advantage via the activation of PGC-1α.

In this study, we investigated the effect of resveratrol on muscle pathology in the dystrophin-deficient mdx mouse. We found that long-term treatment (32 weeks) with resveratrol decreased the ROS levels and attenuated the muscle loss, myofibroblast

JPET Fast Forward. Published on June 7, 2011 as DOI: 10.1124/jpet.111.183210
This article has not been copyedited and formatted. The final version may differ from this version.

differentiation, and abnormal endomysial fibrosis in the mdx mice. Our data suggest that SIRT1 activation may be a useful approach for patients with muscular dystrophies.

Materials and Methods

Animals. All *in vivo* experiments were conducted in strict accordance with *The Guide for the Care and Use of Laboratory Animals*, published by the US National Institutes of Health (NIH publication No. 85-23, revised 1996) and approved by the Animal Use Committee of Sapporo Medical University. Male C57BL/10ScSn-Dmd^{mdx}/J mice (mdx mice) and their control C57BL/10 mice were purchased from Oriental Yeast Co. Ltd. (Tokyo, Japan). Resveratrol was mixed with powdered meal (4 g/kg meal) and orally administered ad libitum to mice for 32 weeks from the age of 9 weeks. The mice were then sacrificed, and the biceps femoris muscles were examined.

Reagents and Antibodies. Resveratrol, TGF-β1, and Hoechst 33342 were purchased from Wako Pure Chemicals (Osaka, Japan). Phalloidin was from Sigma-Aldrich (St. Louis, MO). The antibodies used were anti-acetyl-histone H3 rabbit polyclonal (Calbiochem, San Diego, CA), anti-SIRT1 rabbit polyclonal (Sakamoto et al., 2004), anti-nitrotyrosine mouse monoclonal, anti-Sod2 rabbit polyclonal (Upstate, Lake Placid, NY), anti-8-hydroxy-2'-deoxyguanosine (8-OHdG) mouse monoclonal (Oxis International, Portland, OR), anti-CD45 rabbit polyclonal, anti-p47^{phox} rabbit polyclonal, anti-Nox4 goat polyclonal (Santa Cruz Biotechnology, Santa Cruz, CA), anti-fibronectin sheep polyclonal (Serotec, Oxford, UK), anti-collagen type III rabbit polyclonal (LSL, Tokyo, Japan),

anti-α-smooth muscle actin (α-SMA) mouse monoclonal, anti-GAPDH mouse monoclonal, and anti-α-tubulin mouse monoclonal (Sigma-Aldrich) antibodies. Other reagents were from Wako Pure Chemicals or Sigma-Aldrich.

Immunostaining. Immunostaining was performed as described previously (Tanno et al., 2010). After fixation with 4% paraformaldehyde, samples were blocked with phosphate-buffered saline (PBS) containing 3% bovine serum albumin, 1% goat serum, and 0.1% Triton X-100 (polyethylene glycol p-(1,1,3,3-tetramethylbutyl)-phenyl ether) for 30 min. The samples were then incubated with antibodies against nitrotyrosine (3-Nitro-L-tyrosine; 1:200 dilution), 8-OHdG (1:50 dilution), CD45 (1:50 dilution), α-SMA (1:100 dilution), fibronectin (1: 500 dilution), collagen type III (1:100 dilution), Sod2 (1:500 dilution), acetyl-histone H3 (1:500 dilution), or SIRT1 (1:500 dilution) overnight at 4 °C. The samples were then washed four times with PBS, and incubated with secondary antibodies (1:1000 dilution) overnight at 4 °C. Hoechst 33342 (1:1000 dilution) and phalloidin (1:50 dilution) were used to stain the nucleus and F-actin, respectively. After washing with PBS, the samples were mounted with VECTASHIELD (Vector Laboratories, Burlingame, CA). To compare the expression levels, the fluorescence intensity of an image was quantified by Image-J Software (NIH, Bethesda, MD) and compared among experimental groups. Eight independent images of sections of biceps femoris muscles from each mouse were examined, and the data from

JPET Fast Forward. Published on June 7, 2011 as DOI: 10.1124/jpet.111.183210
This article has not been copyedited and formatted. The final version may differ from this version.

three mice in each group were compared.

Quantitative Reverse Transcription Polymerase Chain Reaction (qRT-PCR). Total RNA was isolated with the RNeasy Fibrous Tissue Mini Kit for muscle tissues or the RNeasy Mini Kit for cultured cells (Qiagen, Valencia, CA). First-strand cDNA was synthesized using SuperScript III (Invitrogen, Carlsbad, CA). DNA amplification was performed in StepOne^{TM} (Applied Biosystems, Foster City, CA) using TaqMan PCR kits for SIRT1, Sod2, β-actin and GAPDH or the Power SYBR Green Master Mix for other genes (Applied Biosystems). The primer sequences were listed in supplemental Table 1.

Western Blotting. Samples were homogenized in CelLytic M Cell Lysis Reagent (Sigma-Aldrich) with 1% protease inhibitor cocktail (Nacalai Tesque, Kyoto, Japan) and centrifuged at 10,000 g for 10 min at 4 °C. The protein concentration of the supernatant was measured using the Protein Quantification Kit-Rapid (Dojindo, Kumamoto, Japan). Supernatant fractions of equal protein concentration were analyzed by Western blotting as described previously (Tanno et al., 2010). The antibodies used were anti-p47^{phox} (1:500), anti-Nox4 (1:200), anti-GAPDH (1:10000), anti-SIRT1 (1:500), anti-acetyl-histone H3 (1:1000), anti-α-SMA (1:400), and anti-α-tubulin (1:2000).

Creatine kinase (CK) and lactate dehydrogenase (LDH) activities. Blood samples obtained by cardiac puncture before the removal of muscular tissues were incubated at room

JPET Fast Forward. Published on June 7, 2011 as DOI: 10.1124/jpet.111.183210
This article has not been copyedited and formatted. The final version may differ from this version.

temperature for 1-2 hr to allow clotting. The samples were then centrifuged at 1,000 g for 10 min, and the supernatants (serum) were stored at -80 ºC until use. The CK and LDH activities were assayed by the Nagahama Life Science Laboratory of the Oriental Yeast Co. Ltd. (Shiga, Japan), and the results were expressed as IU/L.

Cell Culture. C2C12 myoblast cells and L929 fibroblast cells were cultured with Dulbecco's modified Eagle's medium (Wako) supplemented with 1% antibiotic-antimycotic mixed stock solution (Nacalai Tesque) and 10% fetal bovine serum (MP Biomedicals, Solon, OH). Cells were seeded on glass slides for immunocytochemical studies and ROS measurement.

Electroporation of small interfering RNA (siRNA). siRNAs against SIRT1 and control siRNAs were obtained from Sigma Genosys. The siRNAs (100 nM) were electroporated into C2C12 cells twice, 24-hr apart, using the Nucleofector kit (Lonza, Basel, Switzerland). Twenty-four hours after the second transfection, the cells were used for experiments.

Effects of resveratrol on cells. Cells were pretreated with resveratrol (30 μM) or vehicle dimethyl sulfoxide for 3 hr without serum, then TGF-β1 (10 ng/ml) was added to the medium and the cells were further incubated for 24 hr. After washing with PBS, the cells were harvested for qRT-PCR. For immunocytochemistry, the cells were fixed with 4% paraformaldehyde for 10 min.

Analysis of Intracellular ROS Levels. To measure the intracellular ROS levels, cells were

incubated with 5-(and-6)-chloromethyl-2',7'-dichlorodihydrofluorescein diacetate acetyl ester (CM-H_2DCFDA) (Invitrogen) for 30 min at 37 °C and washed twice with PBS. The green fluorescence intensity of the oxidized DCF probe per cell was quantified by Image-J Software and compared among experimental groups. Eight fields of C2C12 cells cultured on a glass disk were examined, and the data from three independent experiments were compared.

Oil Red O Staining. Frozen sections were washed with PBS twice, and fixed with 10% paraformaldehyde for 10 min. After washing with PBS, the sections were washed with 60% isopropyl alcohol, and stained with freshly prepared 0.18% Oil Red O (1-[[2,5-Dimethyl-4-[(2-methylphenyl)azo]phenyl]azo]-2-naphthalenol) in 60% isopropyl alcohol for 20 min. The sections were then rinsed with 60% isopropanol and then with PBS.

Statistical Analysis. Results are presented as means ± SEM, and analyzed by Student's two-tailed t-test for comparisons between two groups, or by one-way ANOVA and the Student-Neuman-Keuls post hoc test for comparisons of three groups. The difference was considered significant if the probability value was <0.05. All analyses were carried out using SigmaStat (Systat, San Jose, CA).

Results

Preservation of Muscle Mass by Resveratrol. Actin staining by phalloidin of the biceps femoris muscles showed a loss of muscle fibers and enlarged interstitial spaces in untreated mdx mice compared with those of control C57BL/10 mice (Fig. 1, A and B). The administration of resveratrol significantly suppressed the myofiber loss and decreased the non-muscle interstitial tissue compared with those of untreated mdx mice (Fig. 1, A and B). qRT-PCR showed that the mRNA levels of myosin heavy chain (MHC) 1, MHC2b, and troponins in the biceps femoris were up-regulated by the administration of resveratrol (Fig. 1, C and D). Skeletal muscles can be divided into type I slow and type II fast fibers. Type I fibers, consisting of proteins such as MHC1 and slow troponin, are able to generate ATP efficiently by oxidative phosphorylation and appear red, whereas glycolytic type II fibers, consisting of proteins such as MHC2b and fast troponin, are white in appearance. The mRNA levels of MHC1 and slow troponin in the muscle from mdx mice fed resveratrol were 5- and 4-fold higher, than those in untreated mdx mice (Fig. 1, C and D). On the other hand, the increase in the mRNA levels of MHC2b and fast troponin were only about 2-fold in the resveratrol-treated mdx mice compared with control mdx mice (Fig. 1, C and D), suggesting that resveratrol affects fiber-type composition of muscles. Consistent with this result, the biceps femoris from the resveratrol- treated mdx mice appeared more red than that of the

JPET Fast Forward. Published on June 7, 2011 as DOI: 10.1124/jpet.111.183210
This article has not been copyedited and formatted. The final version may differ from this version.

control mdx mice (data not shown). However, the number of myofibers in the biceps femoris muscles with central nuclei, indicating newly generated myofibers, was similar in the resveratrol-treated and untreated mdx mice (Figs. 6A and Supplemental Fig. S1A). In addition, the increases in serum CK and lactate dehydrogenase (LDH) levels in the mdx mice were not suppressed by resveratrol treatment (Supplemental Fig. S1, B and C).

Inhibition of Oxidative Stress and Fibrosis by Resveratrol. The biceps femoris of untreated mdx mice displayed high immunoreactivity against anti-nitrotyrosine and anti-8-hydroxy-2'-deoxyguanosine (8-OHdG) antibodies in the interstitial spaces and nuclei, respectively (Fig. 1, E-H), indicating there were high levels of oxidative stress in the muscle tissue. Resveratrol significantly reduced the nitrotyrosine and 8-OHdG immunoreactivities (Fig. 1, E-H).

We next examined the effect of resveratrol on the fibrosis in mdx muscles. The biceps femoris from untreated mdx mice typically showed increased fibrosis in the interstitial spaces of the muscle, indicated by high immunoreactivities against anti-collagen type III and anti-fibronectin antibodies (Fig. 2, A-D). In contrast, resveratrol treatment significantly suppressed the fibrosis and reduced the interstitial spaces (Fig. 2, A-D). The fibronectin, collagen type Ia1, and collagen type Ia2 mRNA levels were significantly higher in the muscles of the mdx mice than in those of control mice. Resveratrol significantly inhibited the

JPET Fast Forward. Published on June 7, 2011 as DOI: 10.1124/jpet.111.183210
This article has not been copyedited and formatted. The final version may differ from this version.

increases in these mRNA levels (Fig. 2, E-G). Myofibroblasts, which may be derived from fibroblasts, are principally involved in the progression of fibrotic events (Barnes and Gorin, 2011). Immunostaining for the myofibroblast marker, α-smooth muscle actin (α-SMA), showed that α-SMA was expressed only in the muscular blood vessels of control C57BL/10 mice, whereas it was also highly expressed in the interstitial tissues of muscles of mdx mice, suggesting that the myofibroblasts promoted the interstitial fibrosis in the mdx mice. (Fig. 2, H and I). Resveratrol significantly decreased the immunoreactivity against the α-SMA antibody in the muscles of the mdx mice (Fig. 2, H and I). In addition, pseudo-hypertrophy of the muscle by adipocyte proliferation is often found in DMD, but no fat deposition was detected by Oil Red O staining in the biceps femoris of the treated or untreated mdx mice (Supplemental Fig. S1D).

Effect of Resveratrol on Inflammatory Responses. Inflammatory cells are often found in the muscle of DMD patients (Emery, 2002). To examine whether the infiltration of inflammatory cells was influenced by resveratrol treatment, we examined the biceps femoris muscles with an antibody against CD45, a leukocyte common antigen. Abundant $CD45^+$ cells were present in the muscles of resveratrol-treated and untreated mdx mice compared with those of control C57BL/10 mice (Fig. 3A). The CD45 mRNA level was also higher in the biceps femoris muscle of the mdx mice than in that of control C57BL/10 mice, and resveratrol

JPET Fast Forward. Published on June 7, 2011 as DOI: 10.1124/jpet.111.183210
This article has not been copyedited and formatted. The final version may differ from this version.

treatment did not reduce the CD45 mRNA expression (Fig. 3B). In addition, the mRNA levels of tissue necrosis factor-α (TNF-α), interleukin-1β (IL-1β), TGF-β1, and TGF-β2 were up-regulated in the muscle of mdx mice compared with that of control mice, and resveratrol treatment failed to reduce these cytokines (Fig. 3, C-F). The expression level of TGF-β3 was similar among these three groups. (Fig. 3G). Thus, resveratrol did not block the infiltration of leukocytes or cytokine release in the mdx muscle.

Effect of Resveratrol on ROS-Producing and Detoxifying Enzymes. NADPH oxidase (Nox) is an enzyme complex consisting of a transmembrane catalytic protein Nox or Duox and its regulatory subunits such as $p22^{phox}$, that generates ROS by transferring an electron from NADPH to molecular O_2 (Lambeth et al., 2007). The Nox family has been shown to be involved in the ROS production in the muscle of mdx mice (Whitehead et al., 2010). qRT-PCR showed that the Nox1, Nox4, Duox1, $p22^{phox}$, and $p47^{phox}$ mRNA levels were up-regulated in the biceps femoris of mdx mice compared with those of control mice. Resveratrol significantly suppressed the induction of the Nox4, Duox1, and $p47^{phox}$ mRNAs (Fig. 4), but not that of the Nox1 and $p22^{phox}$ mRNAs (Fig. 4, A and F). The Duox2 mRNA level was not changed among these three groups (Fig. 5E), and Nox3 expression was not detected in the biceps femoris of any group (data not shown).

JPET Fast Forward. Published on June 7, 2011 as DOI: 10.1124/jpet.111.183210
This article has not been copyedited and formatted. The final version may differ from this version.

Previously, we found that the ROS-detoxifying enzyme, Sod2 (Mn-Sod), was induced by resveratrol in the cardiomyocytes from newborn rats and in the myocardium of TO-2 hamsters (Tanno et al., 2010). We examined the expression levels of the related Sod enzymes in the biceps femoris, and although the Sod1 mRNA level was higher in the mdx mice treated with resveratrol, the levels of Sod2 nor Sod3 mRNA were not (Fig. 5, A-C). Immunostaining also showed that the level of Sod2 protein in the biceps femoris was similar among these three groups (Fig. 5, D and E). We also examined the mRNA levels of other ROS-detoxifying enzymes heme oxygenase 1 (Hmox1) and NAD(P)H quinone oxidoreductase 1 (Nqo1), and components of the rate-limiting enzyme for glutathione biosynthesis; glutamylcysteine ligase modulator (Gclm) and glutamylcysteine ligase catalytic subunit (Gclc). These proteins are induced by various types of cell stress via the activation of transcription factor Nrf2 signaling. The levels of Hmox1 and Nqo1 mRNA were similar in the muscles of control and mdx mice, and resveratrol did not affect their expression (Fig. 5, F and G). Gclm and Gclc were down-regulated in the mdx mice compared with control mice, and resveratrol did not induce their expression (Fig. 5, H and I).

Effect of Resveratrol on SIRT1 and Acetyl Histone H3. Resveratrol is an activator of SIRT1 (Howitz et al., 2003). We next examined the localization of SIRT1 in the biceps femoris, because the nuclear localization of SIRT1 is necessary for resveratrol's

JPET Fast Forward. Published on June 7, 2011 as DOI: 10.1124/jpet.111.183210
This article has not been copyedited and formatted. The final version may differ from this version.

cell-protective function (Tanno et al., 2010). Sarcolemmal membranes of the control and mdx mouse muscles showed high immunoreactivity against the anti-SIRT1 antibody, and no significant change was induced by the administration of resveratrol (Fig. 6A). In addition, the nuclear SIRT1 expression levels in muscle fibers with central nuclei (Fig. 6A, arrowheads) were much lower than those with peripheral nuclei (Fig. 6A, arrows). The mRNA level of SIRT1 as well as SIRT3, another sirtuin located mainly in mitochondria, was similar among these groups (Fig. 6, C and D). Because SIRT1 is a histone deacetylase, we also examined the acetylation level of histone H3 at lysine 9 and lysine14 by immunostaining of the biceps femoris. The nuclei of mdx mice showed higher acetyl histone H3 levels compared with those of control mice, and the administration of resveratrol significantly reduced the acetylation level (Fig. 6B), suggesting that SIRT1 was activated by resveratrol in the muscle of the mdx mice.

Involvement of SIRT1 in the Function of Resveratrol. Resveratrol decreased the ROS levels, fibrosis, and myofibroblastic changes, but it did not suppress the infiltration of inflammatory cells or TGF-β1 production. In C2C12 myoblast cells, TGF-β1 upregulated the ROS levels, fibronectin synthesis, and α-SMA expression, indicating that TGF-β1 gave rise to oxidative damage and induced fibrotic changes in these cells (Fig. 7). Pretreatment with resveratrol reduced the ROS levels (Fig. 7, A and B) and suppressed the fibronectin synthesis

JPET Fast Forward. Published on June 7, 2011 as DOI: 10.1124/jpet.111.183210
This article has not been copyedited and formatted. The final version may differ from this version.

(Fig. 7, E and F) and α-SMA expression (Fig. 7, G and H) triggered by TGF-β1 in C2C12 cells. The upregulation of fibronectin mRNA by TGF-β1 in C2C12 and L929 fibroblast cells was also suppressed by resveratrol (Fig. 7, C and D).

To verify the role of SIRT1, we used SIRT1 siRNA. Among three siRNAs for SIRT1, SIRT1-si(5675) effectively reduced the expression level of SIRT1 mRNA (Supplemental Fig. S2) and was used in the following experiments. Expression of the SIRT1 siRNA elevated the ROS levels and blocked resveratrol's suppressive function on ROS production in C2C12 cells (Fig. 7, A and B), indicating that SIRT1 was involved in the suppression of ROS levels and that resveratrol decreased the oxidative damage via SIRT1. The knockdown of SIRT1 also cancelled the reduction of fibronectin and α-SMA expression by resveratrol (Fig. 7, E-H). Thus, the inhibition of the myofibroblastic change and of fibronectin synthesis by resveratrol also appeared to be mediated by SIRT1 in C2C12 cells.

In the biceps femoris of mdx mice, the α-SMA (Fig. 2, H and I) and acetyl histone H3 levels (Fig. 6B) increased and Nox4 and $p47^{phox}$ were up-regulated (Fig. 4). We found that SIRT1 knockdown with SIRT1 siRNA in C2C12 cells significantly increased the acetyl histone H3 levels, indicating that SIRT1 promoted the deacetylation of histone H3 in these cells (Fig. 8, A and B). Treatment with SIRT1 siRNA also increased the Nox4, $p47^{phox}$, and

α-SMA levels,, demonstrating that SIRT1 downregulated the Nox4, $p47^{phox}$, and α-SMA expression (Fig. 8, A and B).

JPET Fast Forward. Published on June 7, 2011 as DOI: 10.1124/jpet.111.183210
This article has not been copyedited and formatted. The final version may differ from this version.

Discussion

Long-term treatment of mdx mice with resveratrol reduced the myofiber loss (Fig. 1, A-D) accompanied by decreased levels of ROS (Fig. 1, E-H), myofibroblast cells (Fig. 2, H and I), and fibrosis (Fig. 2, A-G) in the muscles. Resveratrol treatment did not affect the infiltration of inflammatory cells or TGF-β1 cytokine release (Fig. 3). This is the first report to demonstrate the significant therapeutic efficacy of a SIRT1 activator, resveratrol, in the dystrophin-deficient mdx mice. Our results also suggest that targeting SIRT1 with pharmacological activators might improve the muscle pathology in patients with muscular dystrophies.

In the biceps femoris of mdx mice, the nitrotyrosine and 8-OHdG levels were high compared to those of control mice, and the administration of resveratrol significantly reduced the oxidative damage (Fig. 2). In addition, the expression levels of some of the subunits of NADPH oxidase, which is involved in ROS production, increased in the biceps femoris of mdx mice, and resveratrol significantly suppressed the levels of Nox4, Duox1, and $p47^{phox}$ (Fig. 4). Previous studies reported the up-regulation of Nox2 in the tibialis anterior muscle (Whitehead et al. 2010) and of Nox4 in the cardiac muscle (Spurney et al., 2008) of mdx mice. The discrepancy in the increased Nox subunits might be due to differences in the muscle examined and in the age of the mice. Duox1 is expressed in the thyroid gland (Lambeth et al.,

JPET Fast Forward. Published on June 7, 2011 as DOI: 10.1124/jpet.111.183210
This article has not been copyedited and formatted. The final version may differ from this version.

2007), and its function in the skeletal muscle is unknown. Nox4 is able to produce ROS without cytosolic regulatory subunits (Lambeth et al., 2007), suggesting that its high expression level may directly increase the ROS level in muscle. Because Nox4 is reported to be involved in several diseases, including heart failure (Kuroda et al., 2010), ischemic stroke (Kleinschnitz et al., 2010), and atherosclerosis (Tong et al., 2010), the decrease in ROS levels by resveratrol treatment may be due in part to the reduction of Nox4 expression in these muscle tissues. Since p47 ^{phox} is a regulator of Nox2 activity (Lambeth et al., 2007), the inhibition of p47^{phox} up-regulation might also contribute to the decreased ROS production in muscle. SIRT1 knockdown increased the expression levels of Nox4 and p47^{phox} (Fig. 8A), indicating that resveratrol decreases the Nox4 and p47^{phox} levels via SIRT1 activation in the biceps femoris of mdx mice.

TGF-β is a multifunctional cytokine that regulates diverse cellular processes, including proliferation, differentiation, apoptosis, and the immune response. We showed that resveratrol decreased the ROS levels and fibrosis, but it did not reduce TGF-β1 level in mdx mice. Our *in vitro* experiments showed that TGF-β1 induced ROS production, myofibroblast differentiation, and fibrotic change in C2C12 cells and that resveratrol significantly suppressed these changes via SIRT1 (Fig. 7). Thus, the suppression of TGF-β1 signaling by SIRT1 may be an important mechanism for resveratrol's activity. TGF-β1 promotes the

JPET Fast Forward. Published on June 7, 2011 as DOI: 10.1124/jpet.111.183210
This article has not been copyedited and formatted. The final version may differ from this version.

acetylation of Smad3, a critical mediator of the TGF-β1 signal, thereby increasing Smad3's activity (Inoue et al., 2007). In contrast, SIRT1 deacetylates and inhibits Smad3 (Li et al., 2010), and thus, the induced deacetylation of Smad3 by resveratrol may be involved in the suppression of TGF-β1 function in the mdx mice. TGF-β1 also induces acetylation of the Rel/p65 subunit of NF-κB and activates NF-κB (Ishinaga et al., 2007). Because SIRT1 inhibits NF-κB by deacetylating Rel/p65 (Yeung et al., 2004), the inhibition of NF-κB by resveratrol via SIRT1 may also have a role in suppressing the signals of TGF-β1 and other cytokines elevated in the muscle of mdx mice. In addition, the infiltration and activation of macrophages in muscle promotes ROS production and has been suggested to be critical for the muscular degeneration in DMD (Desgerre et al., 2009). Because resveratrol suppresses the activity of macrophages via SIRT1 activation (Yoshizaki et al., 2010), it may also stabilize macrophages and inhibit inflammation.

Resveratrol has been shown to prevent cardiac fibrosis in cardiomyopathic hamsters (Tanno et al., 2010) and the renal fibrosis of obstructed mouse kidneys (Li et al., 2010). In the present study, treatment with resveratrol also suppressed the muscular endomysial fibrosis of mdx mice (Fig. 2). Recently Desgerre *et al.* (2009) examined the relationship between the long-term outcome and initial histological alterations for myofiber atrophy, necrosis, fatty degeneration, and endomysial fibrosis in muscle biopsies from patients with DMD.

JPET Fast Forward. Published on June 7, 2011 as DOI: 10.1124/jpet.111.183210
This article has not been copyedited and formatted. The final version may differ from this version.

Interestingly, they found that only endomysial fibrosis was correlated with poor motor outcome and with the age at which loss of ambulation occurred (Desguerre et al., 2009). This finding suggests that the suppression of muscle fibrosis by resveratrol may aid in maintaining the motor function of dystrophy patients.

Differentiation into myofibroblast cells is closely related to fibrosis (Barnes and Gorin, 2011). The apparent reductions in fibrosis and α-SMA expression levels by resveratrol treatment in mdx muscle (Fig. 2) and C2C12 cells (Fig. 7), suggests that the inhibition of myofibroblast differentiation is an important mechanism for the anti-fibrotic action of resveratrol. Nox4 expression has been considered a critical mediator of myofibroblast differentiation and tissue fibrosis (Barnes and Gorin, 2011). Nox4 expression is induced by TGF-β via Smad3 activation (Lambeth et al., 2007; Hecker et al., 2009), while the knockdown of Nox4 suppresses TGF-β-induced α-SMA and fibronectin expression in cardiac and lung fibroblasts (Cucoranu et al., 2005; Hecker et al., 2009). These results indicate that the suppression of Nox4 by resveratrol contributes to reduced ROS levels, myofibroblast differentiation, and fibrosis in the muscle of mdx mice.

The expression levels of the cytoprotective ROS-detoxifying enzymes Sod1, Sod2, and Sod3 were not reduced in mdx mice compared with control C57BL/10 mice, and the administration of resveratrol only induced Sod1 (Figs. 4 and 5). In the cardiomyocytes of

JPET Fast Forward. Published on June 7, 2011 as DOI: 10.1124/jpet.111.183210
This article has not been copyedited and formatted. The final version may differ from this version.

TO-2 hamsters, resveratrol significantly induces Sod2 (Tanno et al., 2010) (Supplemental Fig. S3); the discrepancy may be owing to the different tissues analyzed. Alternatively, downregulation of Sod2 gene by TGF-β (Herrera et al., 2004) may compensate the resveratrol's function on Sod2 transactivation. Previously, we found that SIRT1's cytoprotective effect against oxidative stress is derived, not from its cytoplasmic expression, but from its nuclear expression, which increases the Sod2 level, (Tanno et al., 2010). Because the nuclear localization of SIRT1 is necessary for the induction of Sod2, the lower expression level of SIRT1 in centrally nucleated premature fibers compared to that in mature myocytes (Fig. 6A) may limit the efficacy of resveratrol. Severe stress seems to induce nuclear translocation of SIRT1, but the stress in mdx mice may not be sufficient for nuclear localization of SIRT1. The development and co-administration of an agent that promotes the translocation of SIRT1 from the cytoplasm to the nucleus of a cell may be important for increasing resveratrol's activity.

Nevertheless, we found that resveratrol activated SIRT1-dependent signal cascades, for example to inhibit TGF-β1 signaling and decrease the acetyl histone H3 level (Fig. 6B) in the muscle of mdx mice. The increase in slow muscle type I fibers relative to fast-twitch fibers in the biceps femoris of resveratrol-treated mdx mice (Fig. 1, C and D) also suggests that resveratrol activated SIRT1 and promoted the deacetylation of PGC-1α, which plays central

roles in muscle type switching from type II fibers to type I fibers (Handschin et al., 2007). SIRT1 affects differentiation by regulating transcription factors such as MyoD, FOXOs and NF-κB (Fulco et al., 2003; also see review Horio et al., 2011). Modulation of muscular differentiation and regeneration by resveratrol may also contribute to suppress the myofiber loss (Fig. 1).

Although resveratrol increased the muscle mass (Fig. 1), the high serum CK and LDH levels (Supplemental Fig. S1) indicated that muscle injuries still proceeded in the resveratrol-treated mdx mice. Resveratrol has multiple targets; it is known as a mitochondrial depolarizing agent and an inhibitor of tumor cell growth (Dorrie et al., 2001). The dose of resveratrol used in the present study was 4 g/kg diet, which is the same as in our previous study using the TO-2 hamster (Tanno et al., 2010). The amount of resveratrol taken in by the TO-2 hamsters with heart failure is estimated to be about 80 mg/kg/day (Tanno et al., 2010), while that of the mdx mice in our current study was about 500 mg/kg/day. This 6-fold increase in daily resveratrol intake in the mdx mice compared to the TO-2 hamsters may have affected the experimental comparisons. Furthermore, we used a long-term administration for 32 weeks, which may have enhanced the cytotoxic effect of resveratrol. Because a much lower dose of resveratrol (2.5 mg/kg/day) is reported to be effective for improving the insulin sensitivity of mice fed a high-fat diet (Sun et al., 2007), investigations using lower doses of

resveratrol will help clarify the optimum dose for treating mdx mice.

Unfortunately, we could not analyze the functional parameters in the mdx mice. However, clinical trials investigating the safety and efficacy of resveratrol have already started in patients with metabolic syndrome and type 2 diabetes (http://clinicaltrials.gov/). Cumulative data exist for the safe dosage levels, pharmacokinetics, and adverse effects of resveratrol (Patel et al., 2011). Thus, the use of resveratrol in patients with muscular dystrophies may be acceptable in the clinical setting.

Authorship Contributions.

Participated in research design: Horio, Kuno, Tanno, Miura, Shimamoto and Hori.

Conducted experiments: Hori, Kuno, and Hosoda.

Performed data analysis: Horio, Kuno, and Hori.

Wrote the manuscript: Horio, Kuno, and Hori.

References

Alter J, Lou F, Rabinowitz A, Yin H, Rosenfeld J, Wilton SD, Partridge TA and Lu QL (2006) Systemic delivery of morpholino oligonucleotide restores dystrophin expression bodywide and improves dystrophic pathology. *Nat Med* **12**:175-177.

Asai A, Sahani N, Kaneki M, Ouchi Y, Martyn JA and Yasuhara SE (2007) Primary role of functional ischemia, quantitative evidence for the two-hit mechanism, and phosphodiesterase-5 inhibitor therapy in mouse muscular dystrophy. *PLoS One* **2**:e806.

Barnes JL and Gorin Y (2011) Myofibroblast differentiation during fibrosis: role of NAD(P)H oxidases. *Kidney Int*. **79**:944-956.

Cucoranu I, Clempus R, Dikalova A, Phelan PJ, Ariyan S, Dikalov S and Sorescu D (2005) NAD(P)H oxidase 4 mediates transforming growth factor-beta1-induced differentiation of cardiac fibroblasts into myofibroblasts. *Circ Res* **97**:900-907.

Desguerre I, Mayer M, Leturcq F, Barbet JP, Gherardi RK and Christov C (2009) Endomysial fibrosis in Duchenne muscular dystrophy: a marker of poor outcome associated with macrophage alternative activation. *J Neuropathol Exp Neurol* **68**:762-773.

Disatnik MH, Dhawan J, Yu Y, Beal MF, Whirl MM, Franco AA and Rando TA (1998) Evidence of oxidative stress in mdx mouse muscle: studies of the pre-necrotic state. *J Neurol Sci* **161**:77-84.

Dorrie J, Gerauer H, Wachter Y and Zunino SJ (2001) Resveratrol induces extensive apoptosis by depolarizing mitochondrial membranes and activating caspase-9 in acute lymphoblastic leukemia cells. *Cancer Res* **61**:4731-4739.

Emery AE (2002) The muscular dystrophies. *Lancet* **359**:687-695.

Fulco M, Schiltz RL, Iezzi S, King MT, Zhao P, Kashiwaya Y, Hoffman E, Veech RL and Sartorelli V (2003) Sir2 regulates skeletal muscle differentiation as a potential sensor of the redox state. *Mol Cell* **12**:51-62.

Handschin C, Kobayashi YM, Chin S, Seale P, Campbell KP and Spiegelman BM (2007) PGC-1alpha regulates the neuromuscular junction program and ameliorates Duchenne muscular dystrophy. *Genes Dev* **21**:770-783.

Hecker L, Vittal R, Jones T, Jagirdar R, Luckhardt TR, Horowitz JC, Pennathur S, Martinez FJ and Thannickal VJ (2009) NADPH oxidase-4 mediates myofibroblast activation and fibrogenic responses to lung injury. *Nat Med* **15**:1077-1081.

Herrera B, Murillo MM, Alvarez-Barrientos A, Beltrán J, Fernández M, Fabregat I (2004) Source of early reactive oxygen species in the apoptosis induced by transforming growth factor-beta in fetal rat hepatocytes. *Free Radic Biol Med* **36**:16-26.

Horio Y, Hayashi T, Kuno A and Kunimoto R (2011) Cellular and molecular effects of sirtuins in health and disease. *Clin Sci* **121**:191-203.

Howitz KT, Bitterman KJ, Cohen HY, Lamming DW, Lavu S, Wood JG, Zipkin RE, Chung P, Kisielewski A, Zhang LL, Scherer B and Sinclair DA (2003) Small molecule activators of sirtuins extend Saccharomyces cerevisiae lifespan. *Nature* **425**:191-196.

Huang P, Zhao XS, Fields M, Ransohoff RM and Zhou L (2009) Imatinib attenuates skeletal muscle dystrophy in mdx mice. *FASEB J* **23**:2539-2548.

Inoue Y, Itoh Y, Abe K, Okamoto T, Daitoku H, Fukamizu A, Onozaki K and Hayashi H (2007) Smad3 is acetylated by p300/CBP to regulate its transactivation activity. *Oncogene* **26**:500-508.

Ishinaga H, Jono H, Lim JH, Kweon SM, Xu H, Ha UH, Xu H, Koga T, Yan C, Feng XH, Chen LF and Li JD (2007) TGF-beta induces p65 acetylation to enhance bacteria-induced NF-kappaB activation. *EMBO J* **26**:1150-1162.

Kleinschnitz C, Grund H, Wingler K, Armitage ME, Jones E, Mittal M, Barit D, Schwarz T, Geis C, Kraft P, Barthel K, Schuhmann MK, Herrmann AM, Meuth SG, Stoll G, Meurer S, Schrewe A, Becker L, Gailus-Durner V, Fuchs H, Klopstock T, de Angelis MH, Jandeleit-Dahm K, Shah AM, Weissmann N and Schmidt HH (2010) Post-stroke inhibition of induced NADPH oxidase type 4 prevents oxidative stress and neurodegeneration. *PLoS Biol* **8**:e1000479.

Kuroda J, Ago T, Matsushima S, Zhai P, Schneider MD and Sadoshima J (2010) NADPH

oxidase 4 (Nox4) is a major source of oxidative stress in the failing heart. *Proc Natl Acad Sci U S A* **107**:15565-15570.

Lambeth JD, Kawahara T and Diebold B (2007) Regulation of Nox and Duox enzymatic activity and expression. *Free Radic Biol Med* **43**:319-331.

Li J, Qu X, Ricardo SD, Bertram JF and Nikolic-Paterson DJ (2010) Resveratrol inhibits renal fibrosis in the obstructed kidney: potential role in deacetylation of Smad3. *Am J Pathol* **177**:1065-1071.

Patel KR, Scott E, Brown VA, Gescher AJ, Steward WP and Brown K (2011) Clinical trials of resveratrol. *Ann N Y Acad Sci* **1215**:161-169.

Rodgers JT, Lerin C, Haas W, Gygi SP, Spiegelman BM and Puigserver P (2005) Nutrient control of glucose homeostasis through a complex of PGC-1alpha and SIRT1. *Nature* **434**:113-118.

Rodriguez MC and Tarnopolsky MA (2003) Patients with dystrophinopathy show evidence of increased oxidative stress. *Free Radic Biol Med* **34**:1217-1220.

Sakamoto J, Miura T, Shimamoto K and Horio Y (2004) Predominant expression of Sir2alpha, an NAD-dependent histone deacetylase, in the embryonic mouse heart and brain. *FEBS Lett* **556**:281-286.

Sandri M, Lin J, Handschin C, Yang W, Arany ZP, Lecker SH, Goldberg AL, Spiegelman BM

(2006) PGC-1alpha protects skeletal muscle from atrophy by suppressing FoxO3 action and atrophy-specific gene transcription. *Proc Natl Acad Sci USA* **103**:16260-16265.

Schuler M, Ali F, Chambon C, Duteil D, Bornert JM, Tardivel A, Desvergne B, Wahli W, Chambon P, Metzger D (2006) PGC1alpha expression is controlled in skeletal muscles by PPARbeta, whose ablation results in fiber-type switching, obesity, and type 2 diabetes. *Cell Metab* **4**:407-414.

Spurney CF, Knoblach S, Pistilli EE, Nagaraju K, Martin GR and Hoffman EP (2008) Dystrophin-deficient cardiomyopathy in mouse: expression of Nox4 and Lox are associated with fibrosis and altered functional parameters in the heart. *Neuromuscul Disord* **18**:371-381.

St-Pierre J, Drori S, Uldry M, Silvaggi JM, Rhee J, Jager S, Handschin C, Zheng K, Lin J, Yang W, Simon DK, Bachoo R and Spiegelman BM (2006) Suppression of reactive oxygen species and neurodegeneration by the PGC-1 transcriptional coactivators. *Cell* **127**:397-408.

Sun C, Zhang F, Ge X, Yan T, Chen X, Shi X and Zhai Q (2007) SIRT1 improves insulin sensitivity under insulin-resistant conditions by repressing PTP1B. *Cell Metab* **6**:307-319.

Taniguti AP, Pertille A, Matsumura CY, Santo Neto H and Marques MJ (2010) Prevention of muscle fibrosis and myonecrosis in mdx mice by suramin, a TGF-beta1 blocker. *Muscle Nerve* **43**:82-87.

Tanno M, Sakamoto J, Miura T, Shimamoto K, and Horio Y (2007) Nucleocytoplasmic

shuttling of the NAD^+-dependent histone deacetylase SIRT1. *J Biol Chem* **282**:6823-6832.

Tanno M, Kuno A, Yano T, Miura T, Hisahara S, Ishikawa S, Shimamoto K and Horio Y (2010) Induction of manganese superoxide dismutase by nuclear translocation and activation of SIRT1 promotes cell survival in chronic heart failure. *J Biol Chem* **285**:8375-8382.

Tong X, Hou X, Jourd'heuil D, Weisbrod RM and Cohen RA (2010) Upregulation of Nox4 by TGF{beta}1 oxidizes SERCA and inhibits NO in arterial smooth muscle of the prediabetic Zucker rat. *Circ Res* **107**:975-983.

Whitehead NP, Pham C, Gervasio OL and Allen DG (2008) N-Acetylcysteine ameliorates skeletal muscle pathophysiology in mdx mice. *J Physiol* **586**:2003-2014.

Whitehead NP, Yeung EW, Froehner SC and Allen DG (2010) Skeletal muscle NADPH oxidase is increased and triggers stretch-induced damage in the mdx mouse. *PLoS One* **5**:e15354.

Yeung F, Hoberg JE, Ramsey CS, Keller MD, Jones DR, Frye RA and Mayo MW (2004) Modulation of NF-kappaB-dependent transcription and cell survival by the SIRT1 deacetylase. *EMBO J* **23**:2369-2380.

Yoshizaki T, Schenk S, Imamura T, Babendure J L, Sonoda N, Bae EJ, Oh, DY, Lu M, Milne JC, Westphal C, Bandyopadhyay G and Olefsky JM (2010) SIRT1 inhibits inflammatory pathways in macrophages and modulates insulin sensitivity. *Am J Physiol* **298**:E419-428.

Footnotes

The authors' work was supported by the Ministry of Education, Culture, Sports, Science and Technology of Japan [Grant-in-Aid 22590245, a National Project of Knowledge Cluster Initiative of 2nd stage, “Sapporo Biocluster Bio-S” and the Program for Developing the Supporting System for Upgrading the Education and Research] and the Akiyama Life Science Foundation.

Figure legends

Fig. 1. Preservation of muscle mass and decrease in oxidative stress in the muscle of mdx mice by resveratrol administration. (A) Representative merged images of phalloidin- (F-actin, red) and Hoecst 33342- (nucleus, blue) stained sections of the biceps femoris muscles from control C57BL/10 (Ctrl), untreated mdx (Mdx), and mdx mice treated with resveratrol (Mdx + RSV). (B) Quantification of the muscle-fiber area in the biceps femoris from mice in each group. The fluorescence intensity of an image was measured and compared among the experimental groups. Eight images from each mouse were examined, and the data from three mice in each group were compared. (C, D) The mRNA levels of the myosin heavy chain and troponin genes were measured by qRT-PCR (n = 5 or 6 mice/group). (E, F) Representative images of nitrotyrosine (green)-stained muscle sections in C57BL/10, untreated mdx, and

mdx mice treated with RSV, and their quantification as described in (B). (G, H) Representative images of 8-hydroxy-2'-deoxyguanosine (8-OHdG, red)-stained muscle sections and quantification of the immunostaining in each group. ***P<0.001, **P<0.01, and *P<0.05.

Fig. 2. Inhibition of fibrosis and myofibroblast differentiation in the muscle of mdx mice by resveratrol administration. (A, B) Representative immunofluorescence images of collagen type III (green) in sections of the biceps femoris from control (Ctrl), untreated mdx (Mdx), and mdx mice treated with resveratrol (Mdx + RSV). The intensity of the collagen type III fluorescence was examined as in Fig. 1B, and the quantification from three mice in each group is shown. (C, D) Representative fibronectin immunostaining (green) of muscles, and quantification of the immunostaining in each group. (E, F, and G) The mRNA levels of collagen type Ia1 (E), collage type Ia2 (F), and fibronectin (G) were measured by real-time qRT-PCR (n = 5 or 6 mice/group). (H, I) Representative immunofluorescence images of α-smooth muscle actin (SMA, red) in sections of the biceps femoris from control, untreated mdx, and mdx mice treated with resveratrol, and quantification of the α-SMA staining. ***P<0.001, **P<0.01, and *P<0.05.

JPET Fast Forward. Published on June 7, 2011 as DOI: 10.1124/jpet.111.183210
This article has not been copyedited and formatted. The final version may differ from this version.

Fig. 3. Resveratrol fails to suppress the infiltration of inflammatory cells or up-regulation of cytokines in the muscle of mdx mice. (A) Representative immunostaining images of CD45 (green) in sections of the biceps femoris muscle from control (Ctrl), untreated mdx (Mdx), and resveratrol-treated mdx mice (Mdx + RSV). (B-G) Quantification of the mRNA levels for CD45, tissue necrosis factor-α (TNF-α), interleukin-1β (IL-1β), transforming growth factor-β1 (TGF-β1), TGF-β2, and TGF-β3 in the biceps femoris muscle (n = 5 or 6 mice/group). ***P<0.001, *P<0.05, and n.s. = not significant.

Fig. 4. Resveratrol inhibits the upregulation of NADPH oxidase subunits Nox4, Duox1, and $p47^{phox}$ in the muscle of mdx mice. qRT-PCR of subunits of the Nox family. mRNA levels of the transmembrane catalytic subunits Nox1, Nox2, Nox4, Duox1, and Duox2 (A-E) and the regulatory subunits $p22^{phox}$ and $p47^{phox}$ (F and G) in the biceps femoris muscle (n = 5 or 6 mice/group). The expression levels of Nox 3 were below the detection limit. ***P<0.001, **P<0.01, *P<0.05, and n.s. = not significant.

Fig. 5. Resveratrol up-regulates Sod1, but not other ROS-detoxifying enzymes. (A-C) Quantification of mRNA levels of the superoxide dismutase (Sod) family in the biceps femoris by qRT-PCR (n = 5 or 6 mice/group). (D and E) Representative immunostaining

images of Sod2. Quantification of the Sod2 immunoreactivity was carried out as described in Fig. 1B. (F-G) mRNA levels of heme oxygenase 1 (Hmox1), NAD(P)H quinone oxidoreductase 1 (Nqo1), glutamylcysteine ligase modulator (Gclm), and glutamylcysteine ligase catalytic subunit (Gclc) in the biceps femoris muscle (n = 5 or 6 mice/group). ***P<0.001, **P<0.01, *P<0.05, and n.s. = not significant.

Fig. 6. Resveratrol reduces the acetylation of histone H3 in the muscle of mdx mice. (A and B) Representative immunofluorescence images of the biceps femoris muscle from control (Ctrl), untreated mdx (Mdx), and resveratrol-treated mdx mice (Mdx + RSV) using an anti-SIRT1 antibody (A) and an anti-acetyl-histone H3 antibody that recognizes acetyl lysine residues 9 and 14 in the NH2-terminal region (B). Nuclear staining with Hoechst 33342 is shown in red as a pseudocolor to monitor the colocalization of SIRT1 (green). Yellow (arrows) indicates a high expression level of nuclear SIRT1 in the mature muscle fibers, whereas orange (arrowheads) indicates a low level of SIRT1 in the central nuclei of premature fibers. (C and D) The mRNA levels of SIRT1 (C) and SIRT3 (D) in the biceps femoris muscle were similar among the three groups (n = 5 or 6 mice/group). n.s. = not significant.

Fig. 7. Resveratrol reduces TGF-β1-induced oxidative stress and fibrosis via SIRT1 in C2C12

cells. (A) Representative images of oxidized CM-H_2DCFDA (DCF) in C2C12 cells expressing control (ctrl-si) or SIRT1 siRNA. Cells electroporated with control siRNA (ctrl-si) or SIRT1 siRNA (SIRT1-si) were incubated with or without resveratrol (RSV) for 3 hr, then with vehicle or TGF-β1, and analyzed. (B) The oxidized CM-H_2DCFDA fluorescence was measured as described in Fig. 1B, and compared among experimental groups. The fluorescence intensity of eight fields of C2C12 cells on a glass dish for each group was counted, and the data from three independent experiments were compared. (C and D) qRT-PCR of fibronectin mRNA in C2C12 cells (C) and L929 fibroblasts (D). Cells were incubated with or without resveratrol (RSV) for 3 hr, then with vehicle or TGF-β1, and analyzed (n=3). (E-H) Representative images of fibronectin immunostaining (E) and α-SMA immunostaining (G) in C2C12 cells. The cells were treated as described in (A), and their fluorescence was measured. (F and H) Quantification of fibronectin (F) and α-SMA immunostaining (H). ***P<0.001, **P<0.01, *P<0.05, and n.s. = not significant.

Fig. 8. Knockdown of SIRT1 increases histone H3 acetylation and promotes Nox4, $p47^{phox}$, and α-SMA expression in C2C12 cells. (A) Western blot analysis for SIRT1, acetyl-histone H3, Nox4, $p47^{phox}$, and α-SMA in C2C12 cells expressing control siRNA (ctrl-si) or SIRT1 siRNA (SIRT1-si). Cells were electroporated with each siRNA twice, cultured for another 24

hr, and analyzed. The expression of GAPDH was not affected by the SIRT1 siRNA. (B) Quantitative analysis of the Western blot results from five independent experiments. ***P<0.001, **P<0.01, and *P<0.05.

Fig. 1

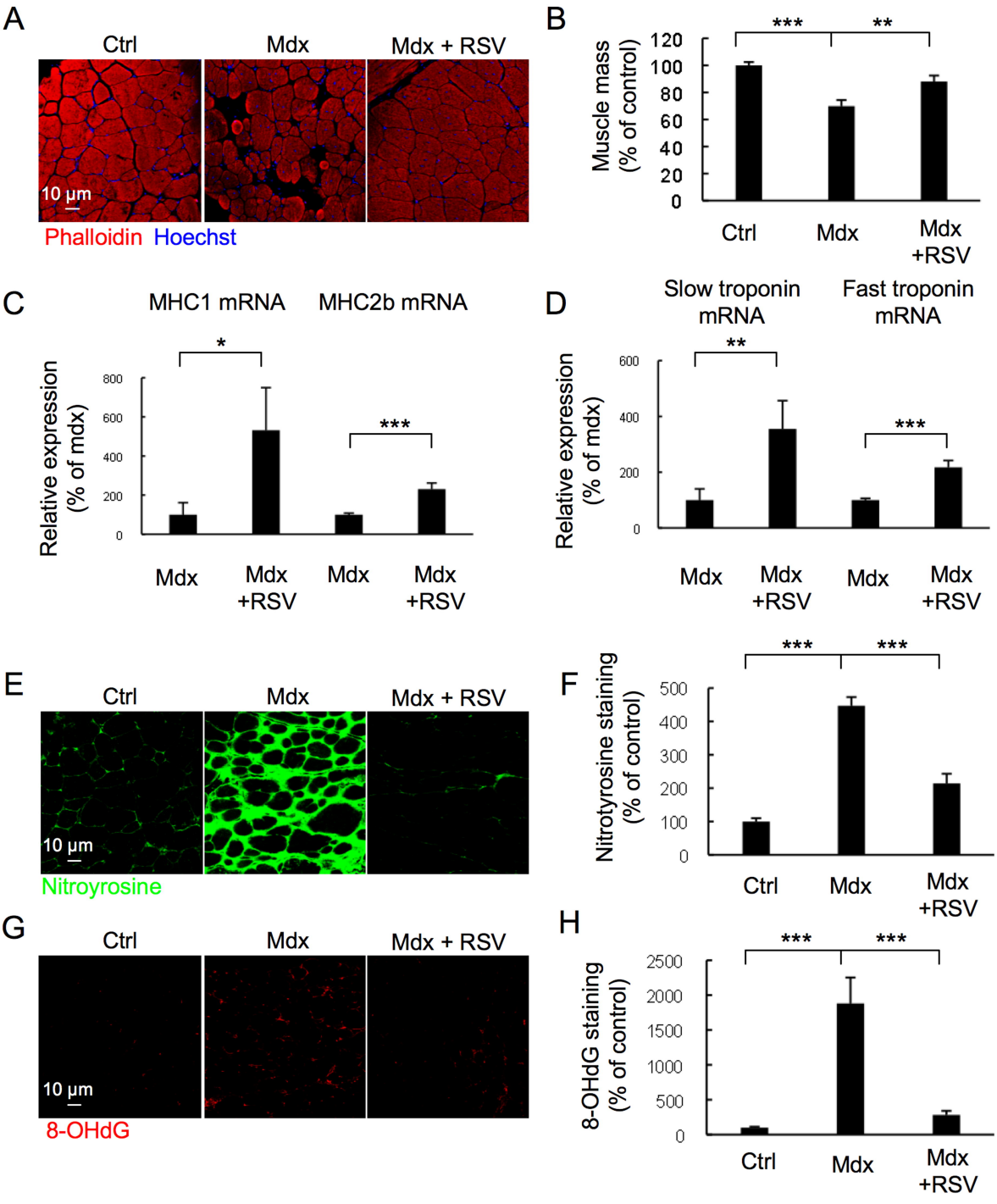
A
Ctrl
Mdx
Mdx + RSV
10 μm
Phalloidin Hoechst
B
Muscle mass (% of control)
120
100
80
60
40
20
0
***
**
Ctrl
Mdx
Mdx +RSV
C
MHC1 mRNA
MHC2b mRNA
Relative expression (% of mdx)
800
600
400
200
0
*
***
Mdx
Mdx +RSV
Mdx
Mdx +RSV
D
Slow troponin mRNA
Fast troponin mRNA
Relative expression (% of mdx)
600
400
200
0
**
***
Mdx
Mdx +RSV
Mdx
Mdx +RSV
E
Ctrl
Mdx
Mdx + RSV
10 μm
Nitroyrosine
F
Nitrotyrosine staining (% of control)
500
400
300
200
100
0
***
***
Ctrl
Mdx
Mdx +RSV
G
Ctrl
Mdx
Mdx + RSV
10 μm
8-OHdG
H
8-OHdG staining (% of control)
2500
2000
1500
1000
500
0
***
***
Ctrl
Mdx
Mdx +RSV

Fig. 2

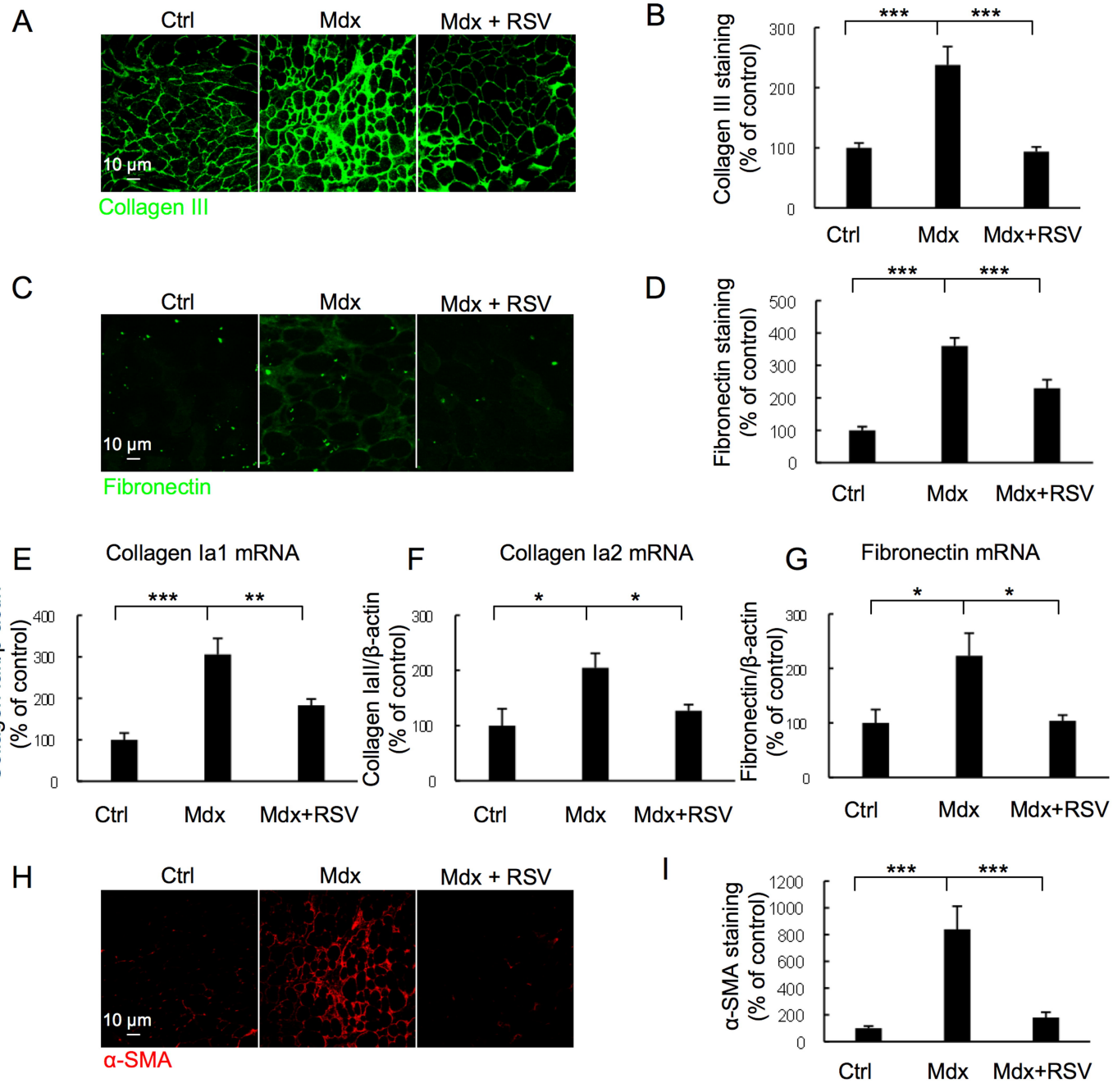
A
Ctrl
Mdx
Mdx + RSV
10 μm
Collagen III
B
Collagen III staining
(% of control)
300
200
100
0
***
***
Ctrl
Mdx
Mdx+RSV
C
Ctrl
Mdx
Mdx + RSV
10 μm
Fibronectin
D
Fibronectin staining
(% of control)
500
400
300
200
100
0
***
***
Ctrl
Mdx
Mdx+RSV
E
Collagen Ia1 mRNA
Collagen Ia1/β-actin
(% of control)
400
300
200
100
0
***
**
Ctrl
Mdx
Mdx+RSV
F
Collagen Ia2 mRNA
Collagen Ia1/β-actin
(% of control)
300
200
100
0
*
*
Ctrl
Mdx
Mdx+RSV
G
Fibronectin mRNA
Fibronectin/β-actin
(% of control)
300
200
100
0
*
*
Ctrl
Mdx
Mdx+RSV
H
Ctrl
Mdx
Mdx + RSV
10 μm
α-SMA
I
α-SMA staining
(% of control)
1200
1000
800
600
400
200
0
***
***
Ctrl
Mdx
Mdx+RSV

Fig. 3

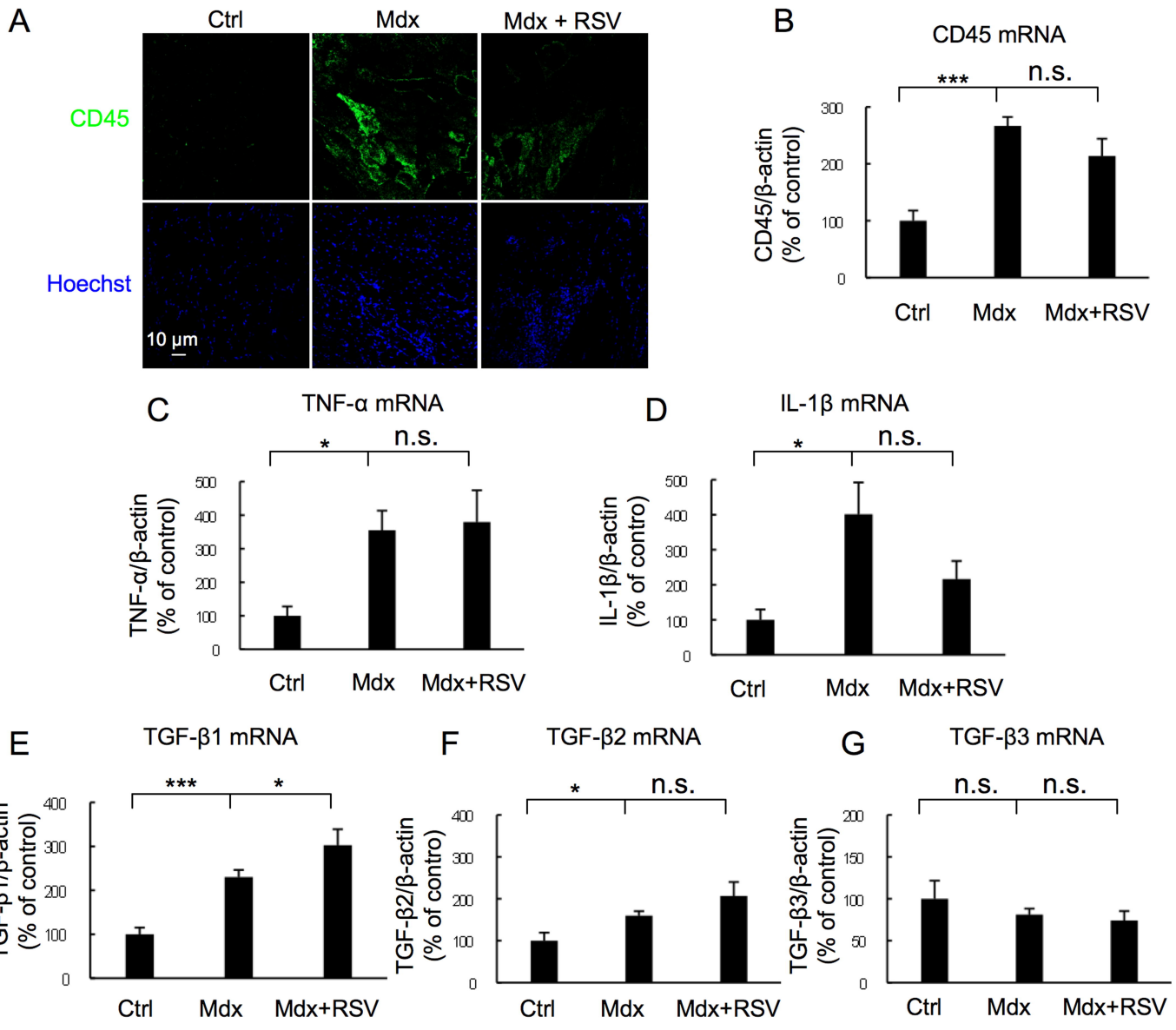
A
Ctrl
Mdx
Mdx + RSV
CD45
Hoechst
10 μm
B
CD45 mRNA
***
n.s.
CD45/β-actin (% of control)
300
200
100
0
Ctrl
Mdx
Mdx+RSV
C
TNF-α mRNA
*
n.s.
TNF-α/β-actin (% of control)
500
400
300
200
100
0
Ctrl
Mdx
Mdx+RSV
D
IL-1β mRNA
*
n.s.
IL-1β/β-actin (% of contro)
500
400
300
200
100
0
Ctrl
Mdx
Mdx+RSV
E
TGF-β1 mRNA
***
*
TGF-β1/β-actin (% of control)
400
300
200
100
0
Ctrl
Mdx
Mdx+RSV
F
TGF-β2 mRNA
*
n.s.
TGF-β2/β-actin (% of contro)
400
300
200
100
0
Ctrl
Mdx
Mdx+RSV
G
TGF-β3 mRNA
n.s.
n.s.
TGF-β3/β-actin (% of control)
200
150
100
50
0
Ctrl
Mdx
Mdx+RSV

Fig. 4

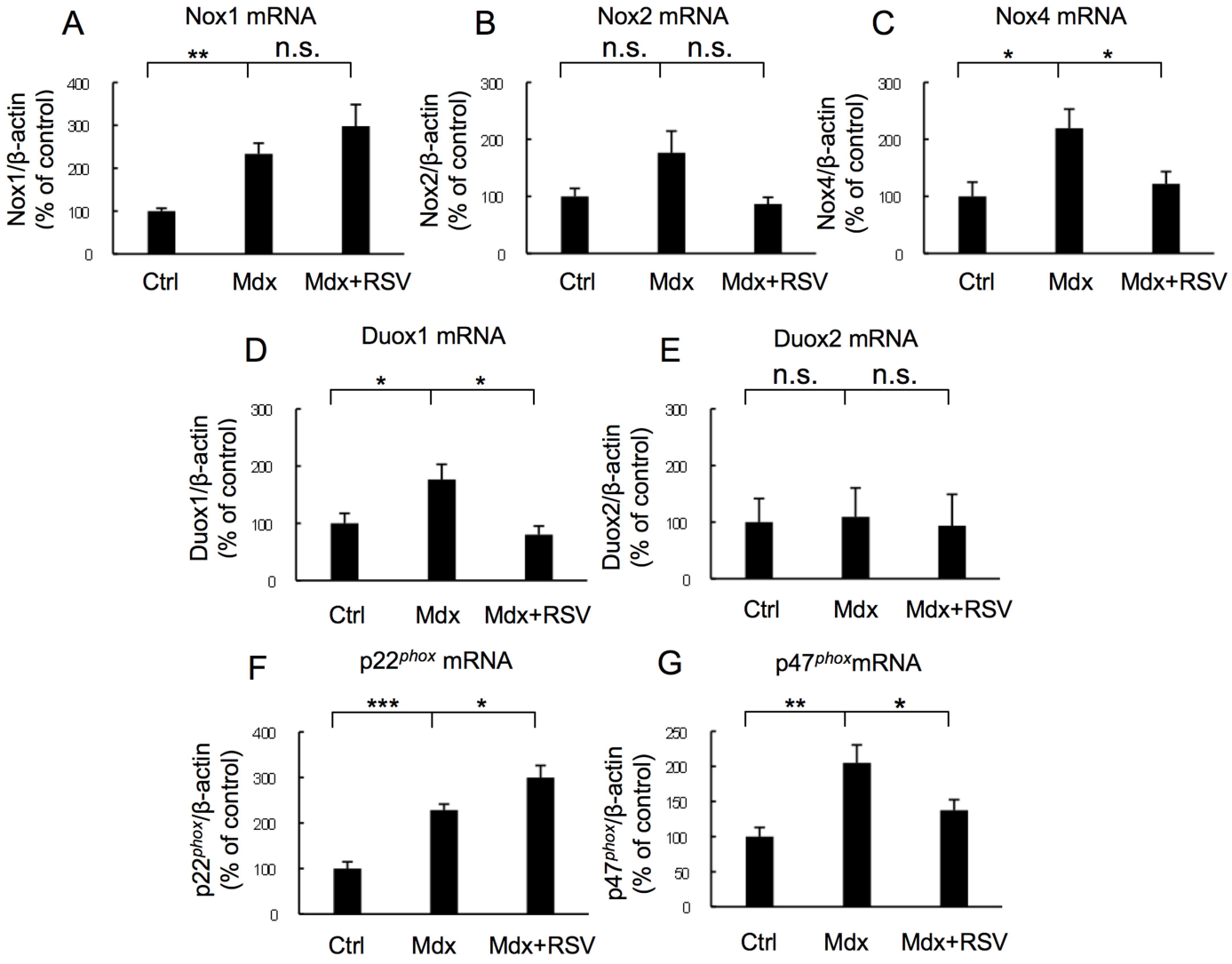
A
Nox1 mRNA
**
n.s.
Nox1/β-actin (% of control)
400
300
200
100
0
Ctrl
Mdx
Mdx+RSV
B
Nox2 mRNA
n.s.
n.s.
Nox2/β-actin (% of control)
300
200
100
0
Ctrl
Mdx
Mdx+RSV
C
Nox4 mRNA
*
*
Nox4/β-actin (% of control)
300
200
100
0
Ctrl
Mdx
Mdx+RSV
D
Duox1 mRNA
*
*
Duox1/β-actin (% of control)
300
200
100
0
Ctrl
Mdx
Mdx+RSV
E
Duox2 mRNA
n.s.
n.s.
Duox2/β-actin (% of control)
300
200
100
0
Ctrl
Mdx
Mdx+RSV
F
p22phox mRNA
***
*
p22phox/β-actin (% of control)
400
300
200
100
0
Ctrl
Mdx
Mdx+RSV
G
p47phox mRNA
**
*
p47phox/β-actin (% of control)
250
200
150
100
50
0
Ctrl
Mdx
Mdx+RSV

Fig. 5

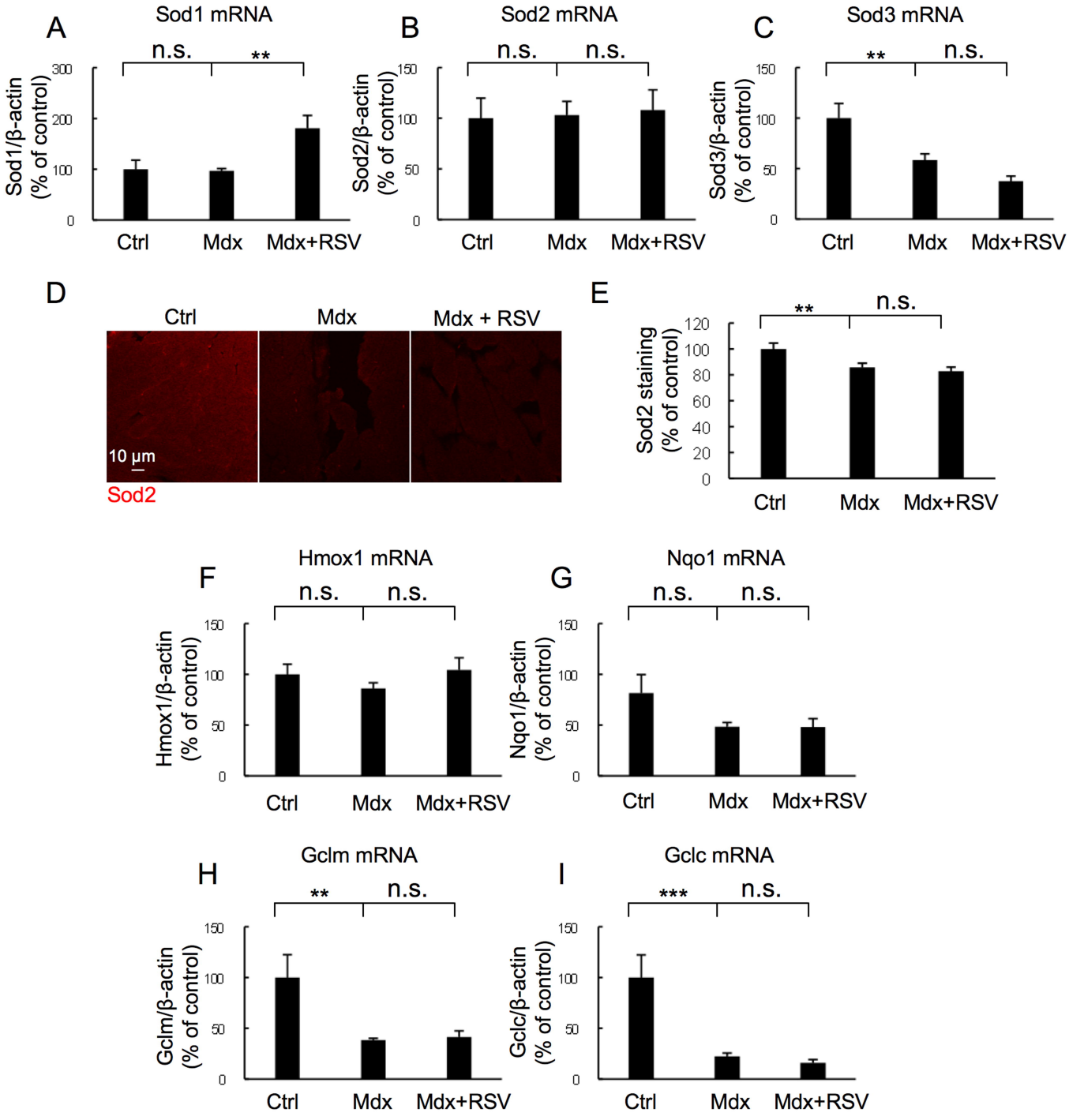
A
Sod1 mRNA
n.s.
**
Sod1/β-actin (% of control)
300
200
100
0
Ctrl
Mdx
Mdx+RSV
B
Sod2 mRNA
n.s.
n.s.
Sod2/β-actin (% of control)
150
100
50
0
Ctrl
Mdx
Mdx+RSV
C
Sod3 mRNA
**
n.s.
Sod3/β-actin (% of control)
150
100
50
0
Ctrl
Mdx
Mdx+RSV
D
Ctrl
Mdx
Mdx + RSV
10 μm
Sod2
E
**
n.s.
Sod2 staining (% of control)
120
100
80
60
40
20
0
Ctrl
Mdx
Mdx+RSV
F
Hmox1 mRNA
n.s.
n.s.
Hmox1/β-actin (% of control)
150
100
50
0
Ctrl
Mdx
Mdx+RSV
G
Nqo1 mRNA
n.s.
n.s.
Nqo1/β-actin (% of control)
150
100
50
0
Ctrl
Mdx
Mdx+RSV
H
Gclm mRNA
**
n.s.
Gclm/β-actin (% of control)
150
100
50
0
Ctrl
Mdx
Mdx+RSV
I
Gclc mRNA
***
n.s.
Gclc/β-actin (% of control)
150
100
50
0
Ctrl
Mdx
Mdx+RSV

Fig. 6

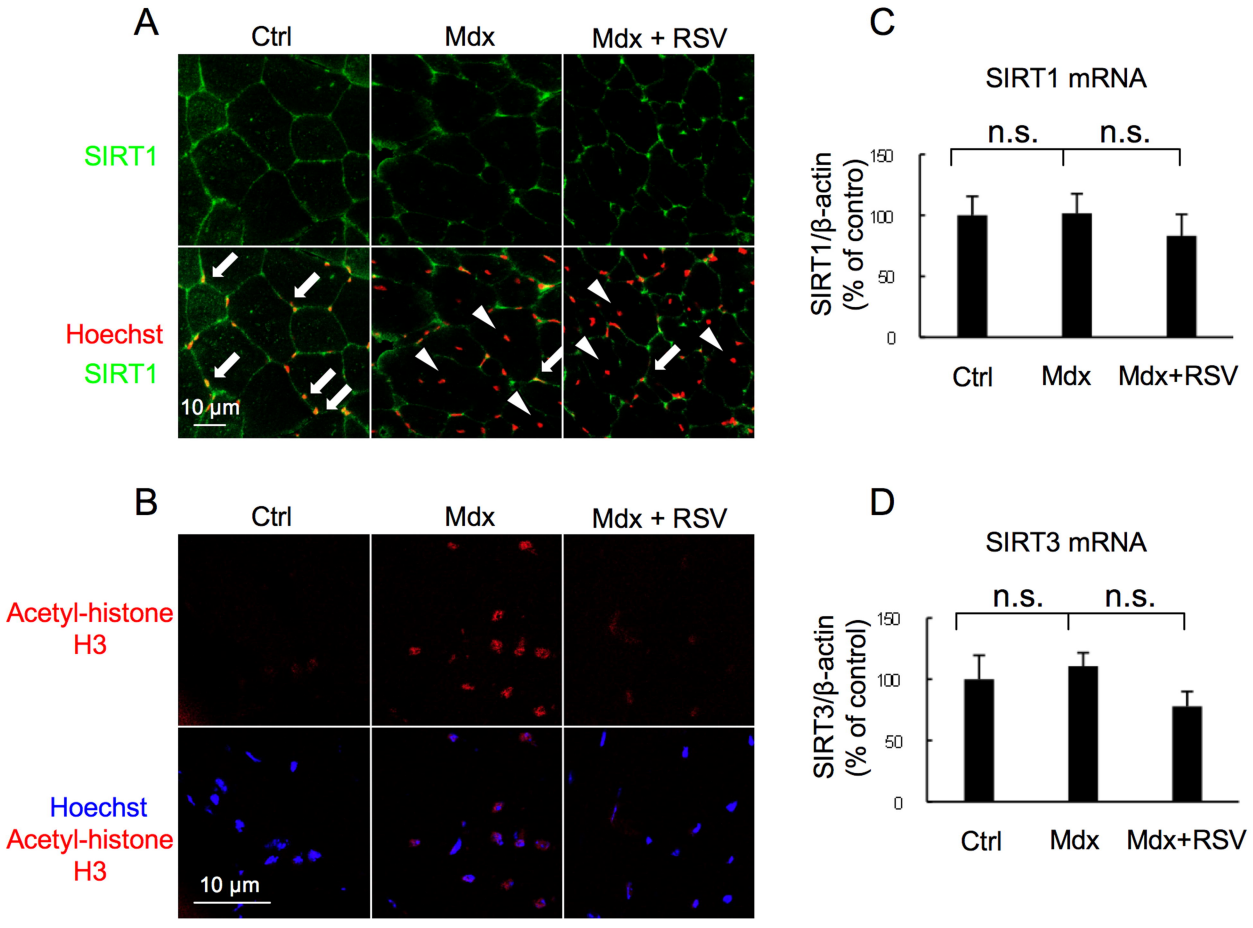
A
Ctrl
Mdx
Mdx + RSV
SIRT1
Hoechst
SIRT1
10 μm
B
Ctrl
Mdx
Mdx + RSV
Acetyl-histone H3
Hoechst
Acetyl-histone H3
10 μm
C
SIRT1 mRNA
n.s.
n.s.
SIRT1/β-actin (% of contro)
150
100
50
0
Ctrl
Mdx
Mdx+RSV
D
SIRT3 mRNA
n.s.
n.s.
SIRT3/β-actin (% of control)
150
100
50
0
Ctrl
Mdx
Mdx+RSV

Fig. 7

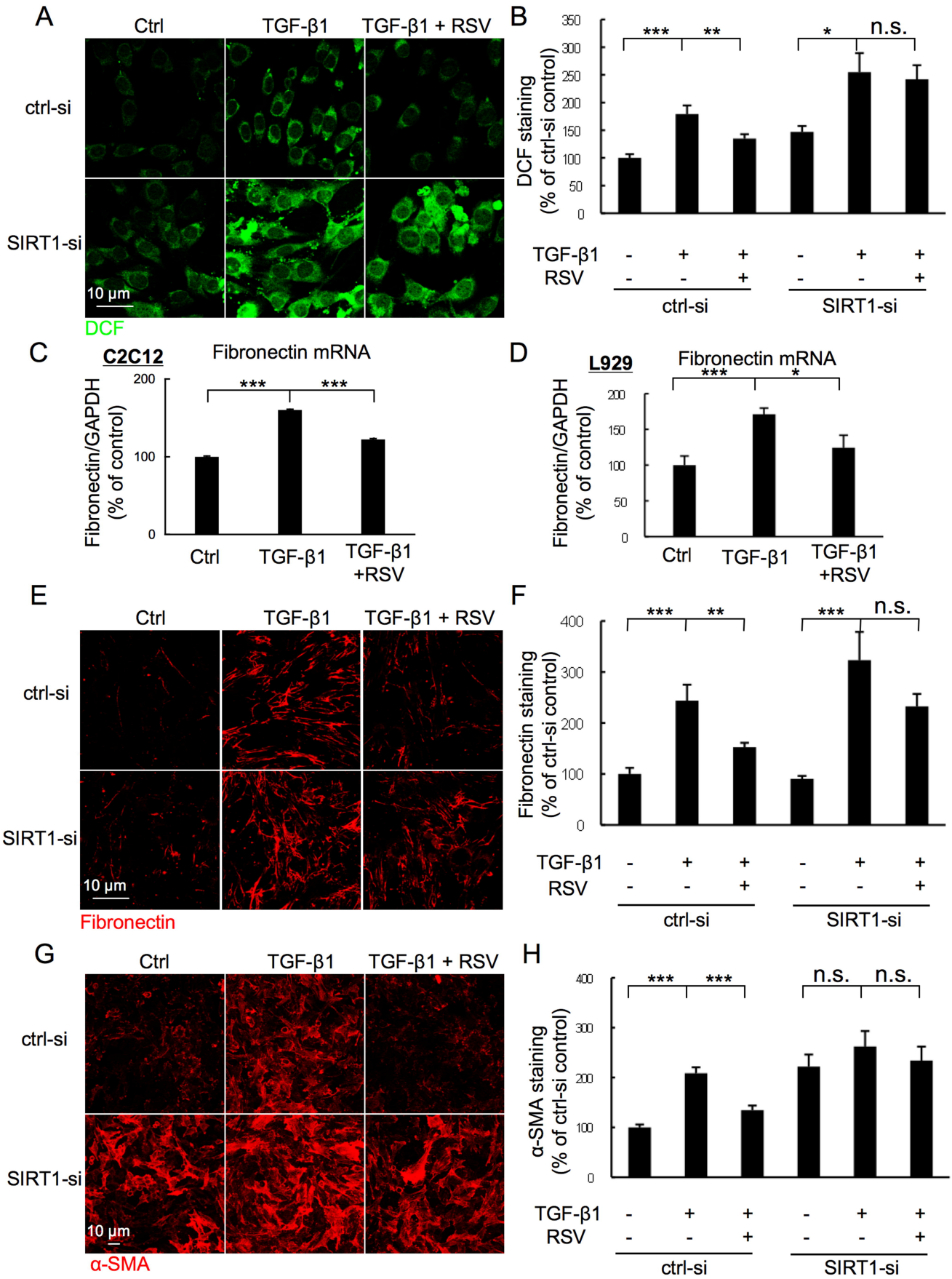
A
Ctrl
TGF-β1
TGF-β1 + RSV
ctrl-si
SIRT1-si
10 μm
DCF
B
DCF staining
(% of ctrl-si control)
***
**
*
n.s.
TGF-β1
RSV
ctrl-si
SIRT1-si
C
C2C12
Fibronectin mRNA
Fibronectin/GAPDH
(% of control)
***
***
Ctrl
TGF-β1
TGF-β1
+RSV
D
L929
Fibronectin mRNA
Fibronectin/GAPDH
(% of control)
***
*
Ctrl
TGF-β1
TGF-β1
+RSV
E
Ctrl
TGF-β1
TGF-β1 + RSV
ctrl-si
SIRT1-si
10 μm
Fibronectin
F
Fibronectin staining
(% of ctrl-si control)
***
**
***
n.s.
TGF-β1
RSV
ctrl-si
SIRT1-si
G
Ctrl
TGF-β1
TGF-β1 + RSV
ctrl-si
SIRT1-si
10 μm
α-SMA
H
α-SMA staining
(% of ctrl-si control)
***
***
n.s.
n.s.
TGF-β1
RSV
ctrl-si
SIRT1-si

Fig. 8

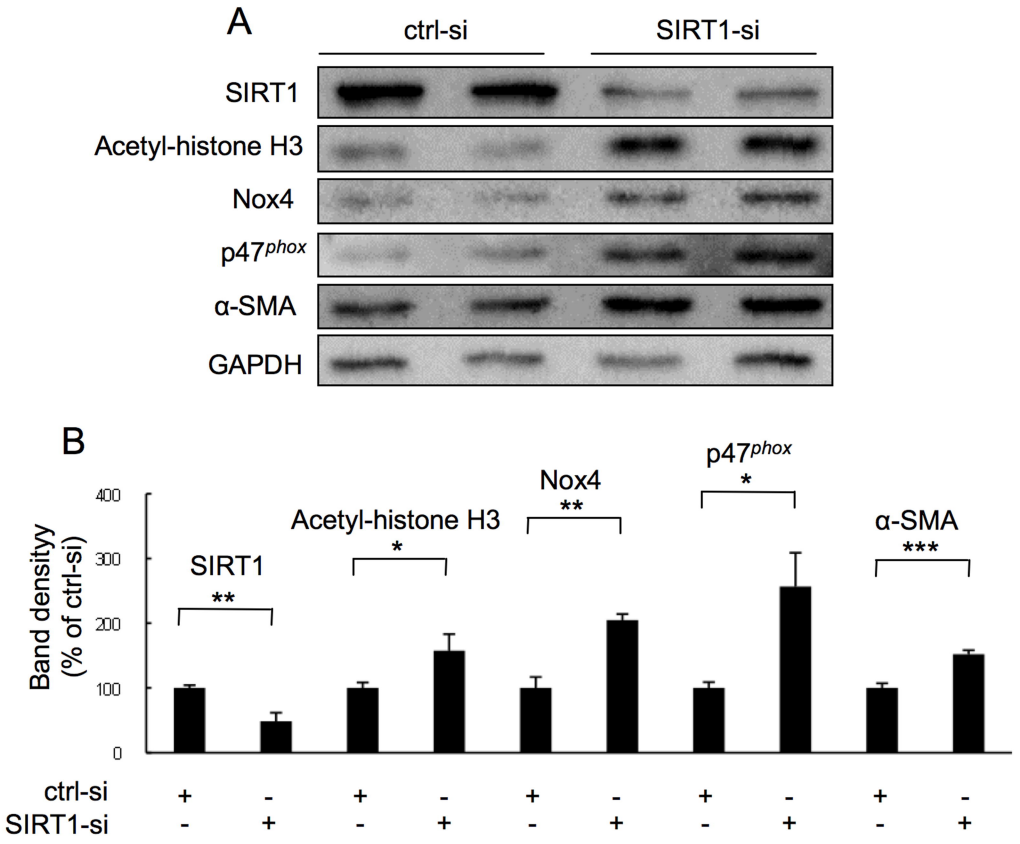
A
ctrl-si
SIRT1-si
SIRT1
Acetyl-histone H3
Nox4
p47phox
α-SMA
GAPDH
B
Band densityy
(% of ctrl-si)
400
300
200
100
0
SIRT1
**
Acetyl-histone H3
*
Nox4
**
p47phox
*
α-SMA
***
ctrl-si
SIRT1-si